BioMetals 1997, **10**, 193–203

Iron uptake and intracellular metal transfer in mycobacteria mediated by xenosiderophores

Berthold F. Matzanke*, Rudolf Böhnke†, Ute Möllmann‡, Rolf Reissbrodt§, Volker Schünemann¶ & Alfred X. Trautwein¶

**Isotopenlabor, Technisch-Naturwissenschaftliche Fakultät, Medizinische Universität, Lübeck, †Mikrobiologie/Biotechnologie, Eberhard-Karls-Universität, Tübingen, ‡Hans-Knöll-Institut für Naturstoff-Forschung (HKI), Jena, §Robert Koch Institut, Wernigerode and ¶Institut für Physik, Medizinische Universität, Lübeck, Germany*

Received 2 August 1996; accepted for publication 4 September 1996

Growth promotion was tested using *M. smegmatis* wild type strain, an exochelin-deficient mutant, and *M. fortuitum* employing a broad variety of xenosiderophores including hydroxamates, catecholates and α-hydroxy carboxylic acids. The experiments revealed that utilization of siderophore-bound iron is substrate specific suggesting high-affinity siderophore receptor and transport systems. Concentration-dependent uptake of a selected xenosiderophore (fericrocin) in *M. smegmatis* showed saturation kinetics and uptake was inhibited by respiratory poisons. *In situ* Mössbauer spectroscopy of ferricrocin uptake in *M. smegmatis* indicated rapid intracellular reductive removal of the metal excluding intracellular ferricrocin accumulation. The ultimate intracellular iron pool is represented by a compound (δ = 0.43 mm s^{-1}, ΔE_Q = 1.03 mm s^{-1}) which has also been found in many other microorganisms and does not represent a bacterioferritin, cytochrome or iron–sulfur cluster. By contrast, iron uptake via citrate – a compound exhibiting a very low complex stability constant – involves ligand exchange with mycobactin. Mycobactin has merely a transient role. The ultimate storage compound is an *E.coli*-type bacterioferritin, in which over 90% of cellular iron is located.

Keywords: EPR, iron transport, Mössbauer spectroscopy, mycobacterium, xenosiderophores

Introduction

Mycobacteria are the causative agents of a spectrum of human diseases. Due to AIDS, poverty and migration, a drastic worldwide rise of mycobacterial infections is observed (Bloom 1992, Zhang *et al.* 1992, Kaufmann & van Emden 1993, WHO 1993). In addition, an increasing resistance to available tuberculostatic agents has been reported (David 1981, Rastogi 1993). This development urgently demands the search for novel agents and novel targets in the treatment of mycobacterial infections. We have focused our interest on iron transport and metabolism of mycobacteria as a possible basis for antibiotic vectors and novel drug targets.

Iron has attained a central role for the metabolism of most microorganisms. However, the extreme insolubility of ferric ions at neutral pH (K_{SP} = $10^{-38.7}$ M) severely restricts the bioavailability of iron (Neilands 1982, Raymond *et al.* 1984, Matzanke 1991). The same holds for the human host where iron is mainly bound to hemoglobin in erythrocytes, and to transferrin and ferritins in body fluids. Thus microbes have evolved iron complexing agents termed siderophores which are synthesized under conditions of iron deficiency (Neilands 1982, Winkelmann 1986, 1991, Matzanke *et al.* 1989a). It is well documented that many microorganisms exhibit a concomitant response to low-iron stress, namely the synthesis of several outer-membrane

Address for correspondence: B.F. Matzanke, Medizinische Universität zu Lübeck, Isotopenlabor, Technisch-Naturwissenschaftliche Fakultät, Ratzeburger Allee 160, 23538 Lübeck, Germany. Tel: (+49) 451 5004140; Fax: (+49) 451 5004214; e-mail: matzanke@physik.muluebeck.de.

proteins which are essential for specific transport of a variety of siderophores, including those that are synthesized by the organism (endogenous siderophores) or those which are produced by other microorganisms (exogenous or xenosiderophores) (Müller *et al.* 1984, Ecker *et al.* 1986, Bagg & Neilands 1987, Hall *et al.* 1987, Braun & Hantke 1991). This multitude of siderophore transport systems reveals that an enormous effort is devoted by microbial systems to provide sufficient iron for growth.

In mycobacteria membrane-bound (mycobactins) and extracellular (exochelin MS and MN) siderophores have been identified (Ratledge 1964, 1982, Snow 1970, Macham & Ratledge 1975, Barclay & Ratledge 1983, Sharman *et al.* 1995a,b). The irontransport mechanism of the endogenous siderophores is not fully understood (Ratledge & Chaudrey 1971, Ratledge & Hall 1971, Macham *et al.* 1975, Stephenson & Ratledge 1979, Ratledge *et al*. 1982, Hall & Ratledge 1987, Wheeler & Ratledge 1994). Moreover, very little is known about xenosiderophore transport and intracellular iron transfer pathways in this family of Gram positive rods (Ratledge & Chaudrey 1971, Ratledge & Hall 1971, Messenger & Ratledge 1982). In this paper it is shown that a variety of xenosiderophores is utilized by mycobacteria. The data suggest uptake via specific receptor and transport systems.

In addition, we have employed non-destructive *in situ* Mössbauer and EPR spectroscopy to yield information about metal transfer and the main components of iron metabolism, as well as their time-dependent changes. The usefulness of these non-destructive methods has been demonstrated in various investigations (Matzanke 1987, 1991, Matzanke *et al.* 1986, 1989a,b, 1991a,b). Direct evidence is presented for different intracellular iron transfer pathways depending on the xenosiderophore employed.

Materials and methods

Chemicals

Ethylenediaminetetraacetic acid Na_4-salt (EDTA), XAD-2 and Servacel CM–32 were purchased from SERVA (Heidelberg, Germany), CHELEX 100 and Biogel P2 from Biorad (Munich, Germany). ^{57}Fe (95% isotopically pure) was from Wissenschaftliche Elektronik GmbH (Starnberg, Germany). Bovine serum albumine (BSA), chrome azurole S (CAS) and ethylenediamine-di(*o*-hydroxyphenylacetic acid) (EDDHA) were from Sigma Chemical Co. (St. Louis, MO, USA). All other reagents were of analytical grade and purchased from Merck (Darmstadt, Germany). Cellulose nitrate filters (0.45 μm) were from Sartorius (Göttingen, Germany), and Delrin rods were from E.I. du Pont de Nemours & Co., Inc. (Wilmington, DE, USA). Delrin Mössbauer sample holders were manufactured in the machine shop of the corresponding author's institute. Doubly distilled water was used throughout. All glassware used during the experiments was washed with KOH, HCl, EDTA and triply rinsed with water to eliminate adventitiously bound iron.

Siderophores, desferri-siderophores and labelled siderophores

Ferrichrome, rhodotorulic acid, coprogen and rhizoferrin were kindly provided by Professor Winkelmann, University of Tübingen, Germany. Ferrioxamines B and G were obtained from Dr H.H. Peter, Ciba, Basel, Switzerland. Serratiochelin, chrysobactin and pyoverdin were gifts from Professor Budzikiewicz, University of Cologne, Germany. Azotobactin was kindly provided by Dr M.A. Abdallah, University Strasbourg, France. Mycobactin J was purchased from Rhône Mèrieux, Lyon, France. Ferricrocin was isolated from culture supernatants of *Aspergillus viridi-nutans* Ducker and Thrower (CBS 127.65) under the same conditions as described for *Neurospora crassa* (Wong *et al.* 1983). Ferricrocin was purified by column chromatography on Amberlite XAD-2, Servacel CM-32 and Biogel P2. Purity was checked by HPLC, performed on a Nucleosil reversed-phase C_{18} column [5μm, 125 × 4.6 mm; gradient system: double distilled water/acetonitrile (6–40%, trifluoracetic acid 0.1% (v/v), flow rate 1 ml min^{-1}, ramp 19 min, r_t = 12.57 min]. Ferrioxamine G was prepared and purified according to Reissbrodt *et al.* (1990). Mycoexochelin was isolated from *M. smegmatis* SG 987 cultures according to Sharman *et al.* (1995b). Enterobactin was isolated from *E.coli* AN311 using the protocol of Neilands & Nakamuro (1991). Aerobactin was prepared according to Braun (1981) employing an aerobactin-producing *E.coli* wild-type strain. Myxochelin C obtained by organic synthesis was a gift from Professor Trowitzsch-Kienast, FHS Berlin, Germany (Trowitzsch-Kienast *et al.* 1994). Rhizoferrin was kindly provided by Professor Winkelmann, University of Tübingen, Germany (Thieken & Winkelmann 1992). α-2,3-Dihydroxybenzoic acid (DHBA), citric acid and salicylic acid were purchased from SIGMA, Deisenhofen, Germany. Desferri-ferricrocin was prepared by the 8-hydroxyquinoline method (Wong *et al.* 1983). [^{55}Fe]-labelled ferricrocin was prepared by adding a solution of desferri-ferricrocin (30 μl, 10 mM) and [^{55}Fe]Cl_3 (30 μl, carrier-free, in 0.1 M HCl, 0.6 mCi ml^{-1}, Amersham, UK) to a solution of unlabelled ferricrocin (1ml, 10 μmol ml^{-1}). A [^{57}Fe](III) stock solution was obtained by dissolving metallic [^{57}Fe] in a small volume of HNO_3/HCl (1:2 [vol/vol]). The pH of the solution was adjusted to 1.0 with KOH and the Fe(III)-concentration determined spectrophotometrically with desferrioxamine B at A_{428}. Synthesis of [^{57}Fe]ferricrocin was achieved by mixing equimolar solutions of [^{57}Fe](III) and aqueous desferri-ferricrocin. The red-brown reaction product was passed

through a XAD-2 column and sterile filtered. Purity was checked with thin-layer chromatography on silica gel (chloroform/methanol/water (65/25/4), R_f= 0.55). Due to the low complex formation constant [^{57}Fe](citrate)$_2$ was prepared by mixing [^{57}Fe](III) stock solution with a twenty-fold excess of ligand. Complex formation was completed after autoclaving.

Bacterial strains and growth conditions

Mycobacterium smegmatis SG 987 (= HKI 0056, from the institute's culture collection) and *Mycobacterium fortuitum* ATCC 6841 (type strain) are wild type strains. *M. smegmatis* 987-M10 is an exochelin-suppressed mutant of HKI 0056 (this work). Bacteria were maintained on nutrient broth (NB) agar slants (DIFCO). Precultures were grown in baffled Erlenmeyer flasks with gentle shaking at 37ºC in NB medium (per litre: NB, 8 g; NaCl, 5 g). The same conditions were employed for growth in mineral salts medium (MM) which was prepared according to Hall and Ratledge (1982) supplemented (per litre) with $ZnSO_4 \times 7H_2O$, 2.02 mg; $MnSO_4 \times 4H_2O$, 0.4 mg; $MgSO_4 \times 7H_2O$, 0.4 g. For uptake studies cells were grown in low-iron mineral salts medium. Glass beads were added in order to minimize the formation of aggregates. The iron concentration of the medium and of the glycerol stock solution was kept at approximately 10^{-6} M by passing the solutions separately through a CHELEX 100 column to remove Fe^{3+}. An alternative route to make the mineral salts medium iron-deficient was to add EDDHA, a strong iron chelator which cannot be utilized by mycobacteria. This method has been used for the growth promotion tests.

The growth promotion medium used consisted of MM with following additions (per litre): $CaCl_2 \times 2H_2O$, 1 mg; $NaMoO_4 \times 2H_2O$, 0.2 mg; $CuSO_4 \times 2H_2O$, 0.2 mg; $CoCl_2 \times 2H_2O$, 0.4 mg; 12 g agar (Oxoid No.1); 0.8 ml Tween 80; 20 μmol EDDHA. The starvation medium consisted of saline containing (per litre): glycerol, 50 ml, Tween 80, 0.5 ml.

CAS agar medium for detection of siderophore production was prepared as described by Schwyn & Neilands (1987).

Mutagenesis

M. smegmatis HKI 0056 was grown in 100 ml mineral salts medium at 37ºC and 250 rpm to late log phase, harvested by centrifugation and washed with sterile distilled water. The pellet was resuspended in MM yielding a cell density of about 10^9 bacteria per ml. The medium contained *N*-nitrosomethyl-urea (NMU; 1.5 mg ml^{-1}). Cells were cultured with gentle shaking for 60 min at 37ºC. Without time for phenotypic expression cells were plated on NB agar. Screening for exo-siderophore deficient mutants was achieved by inoculating CAS agar plates with colonies. Production of exo-siderophores was indicated by an orange halo around CAS-plate colonies. Mutant 987-M10 was isolated out of 1800 colonies tested. Colonies of 987-M10 exhibited no halo, indicating a lack of exo-siderophores. After about ten days of cultivation a very small halo appeared. The reason for this is not clear. In further studies this mutant will be characterized genetically. It should represent a suitable system for siderophore uptake studies because ligand exchange processes between exochelins and xenosiderophores, which might obscure transport measurements, can be excluded by the cultivation times of the experiments, and also by the negligible amounts of exo-siderophore appearing after that time.

Growth promotion and cross-feeding tests

Mycobacteria were cultivated on NB agar (12 g agar Oxoid No.1 per litre) at 37ºC for 48 h and were then suspended in starvation medium. At a cell density of approximately 3×10^8 cells per ml (optical density of McFarland No.1) 1.5 ml of the cell suspension were mixed with growth promotion medium to give a final volume of 100 ml and the resulting suspension was poured into Petri dishes. According to Reissbrodt *et al.* (1993) 5 μg natural siderophore or synthetic iron chelates were applied on filter discs and dried. On each Petri dish a mycobactin containing disc (2 μg per disc) was placed in the centre, surrounded by six discs loaded with other iron chelators. The growth zones were measured after 24 h incubation at 37ºC and after four additional days of growth at room temperature.

Transport experiments

Cells were taken from agar slants and grown in NB medium for five days. Cells were then transferred to mineral salts medium (2% inoculum) and grown for an additional five days. Taking a 5% inoculum of this culture, the mycobacteria were cultivated for six days in iron-deficient MM, washed by centrifugation, resuspended in fresh medium and grown for an additional 4 h. Aliquots of this suspension were taken for the transport assays. Transport was started by the addition of various quantities of [^{55}Fe]ferricrocin (specific activity 2.2 kBq nmol^{-1}). Samples (1 ml, corresponding to approximately 1.2 mg dry mass) were taken at 30 min intervals over a time range of 3 h, filtered on cellulose nitrate membrane filters (0.45 μm) and washed twice with ice-cold 0.9% LiCl solution. The radioactivity on the filters was measured in a liquid scintillation counter.

Mössbauer measurements

For Mössbauer measurements the sequence of growth processes was the same as in the [^{55}Fe] transport experiments. However, more medium (2 l in baffled 5 l Erlenmeyer flasks) was required in order to obtain sufficient cell material (approximately 1 cm^3 of packed cells). After six days of growth in iron-deficient mineral salts medium 20μM [$^{57}Fe^{3+}$]ferricrocin or [$^{57}Fe^{3+}$](citrate)$_2$ was added to the cell suspension. After 2 h incubation, cells were cooled down to 4ºC within two minutes, washed, and transferred to Delrin Mössbauer sample holders. All sample volumes were about 1 ml. Sample thickness did not exceed 9 mm.

The containers were quickly frozen in liquid nitrogen and kept in a liquid nitrogen storage vessel until measurements were completed. In a second set of Mössbauer experiments the inoculum was supplied with [^{57}Fe]chelate and the cultures were grown for six days. Mössbauer samples were prepared as described above.

The Mössbauer samples were either frozen cells or frozen solutions. The Mössbauer spectra were recorded in the horizontal transmission geometry using a constant acceleration spectrometer operated in conjunction with a 512-channel analyser in the time-scale mode. The source was at room temperature and consisted of 1.85 GBq [^{57}Co] diffused in Rh foil (Amersham Buchler, Braunschweig, Germany). The spectrometer was calibrated against a metallic α-iron foil at room temperature yielding a standard line width of 0.24 mm s^{-1}. The Mössbauer cryostat was a helium bath cryostat (MD306, Oxford Instruments, Oxon, UK). A small field of 20 mT perpendicular to the γ-beam was applied to the tail of the bath cryostat using a permanent magnet. Isomer shift δ, quadrupole splitting ΔE_Q, and percentage of the total absorption area were obtained by least-squares fits of Lorentzian lines to the experimental spectra.

EPR spectroscopy

Measurements were made at X-band (9.4 GHz) using a cw-EPR spectrometer (Bruker ER200D SRC) equipped with a helium-flow cryostat (Oxford Instruments ESR9110). The data acquisition system, based on a personal computer, is our own development.

Results and discussion

Growth promotion tests

In an initial screening, growth promotion of *M. smegmatis* SG 987 and its exochelin mutant 987-M10, and of *M. fortuitum* was tested on a variety of siderophores and iron chelating agents including hydroxamates and catecholates, as well as α-hydroxy carboxylic acids. The results are shown in Table 1. The siderophores serratiochelin, myxochelin, ferricrocin, rhodotorulic acid, mycobactin and mycoexochelin MS gave excellent growth response in all three organisms (growth diameters > 20 mm). Ferrioxamine B, rhizoferrin, citrate and salicylic acid yielded good growth promotion (growth zone diameters 12–20 mm). All other compounds tested resulted in little or no growth promotion at all. These experiments clearly demonstrate that utilization of siderophore-bound iron is associated with substrate specificity.

The ligands employed in the growth promotion tests exhibit a wide range of different structural building blocks. Moreover, the stability constants of these Fe–siderophore complexes vary considerably. One measure for the stability of the complexes is the pM-value which is defined as follows: pM = –log[$Fe(H_2O)_6^{3+}$], when $[Fe]_T = 10^{-6}$ M, and ligand $[L] = 10^{-5}$ M at pH 7.4. The pM value of enterobactin is 35.5; of ferricrocin 26.5; of aerobactin 23.3; of rhodotorulic acid 21.9; and of citrate 17.7 (Raymond *et al.* 1984). For mycobactins no stability constants are known. Based on the ligands employed in iron binding (two hydroxamates, a phenolate and an oxazoline nitrogen), a pM value between 23 and 26 should be expected for mycobactins ($\log \beta_{110} \approx 30$, estimated by Snow, 1970) whereas for exochelin MS a complex stability constant in the range 25 to 27 is likely. The structural and thermodynamic variety of the growth promoting siderophores suggests specific uptake systems. Moreover, diffusion-controlled processes cannot account for the observed differences of growth promotion of similar siderophores like ferrichrome/ferricrocin ($\log \beta_{110}$ 29.1/30.4) or enterobactin/myxochelin ($\log \beta_{110}$ 52 $\geqslant$ 40) (Raymond *et al.* 1984). The β_{110}-value of myxochelin has not yet been determined. However, no value below 40 has so far been found for triscatecholate ligands. From this we conclude that there exists – similar to other bacteria – a variety of different and very substrate-specific iron accumulation pathways of xenosiderophores in mycobacteria. This in turn requires high-affinity receptors and transport systems.

Growth of the exochelin mutant 987-M10 on citrate, salicylic acid, rhizoferrin and ferrioxamine B resulted in decreased growth promotion compared to the wild type strain. This finding implies that ligand exchange with exochelin accounts – at least in part – for the iron uptake process from these substrates. The low stability constants of ferric citrate, salicylate and rhizoferrin fit this model; however, in the case of ferrioxamine B this explanation falls short.

After prolonged incubation a sharp secondary growth zone could be observed in some of the growth promotion tests (marked by asterisks in Table 1). This was located between the siderophore disc and the mycobactin disc (cross-feeding). The rationale for this secondary growth zone is not yet clear and remains to be elucidated in a future investigation.

[^{55}Fe] transport studies

For a detailed study of uptake kinetics and iron metabolism in *M. smegmatis* we have selected the cyclic hexapeptide siderophore ferricrocin because this compound seemed to be a promising candidate

Table 1. Growth promotion tests of mycobacteria on low-iron agar. Siderophores were added on filter discs and growth zones were measured after 24 h of incubation at 37°C. +: growth zones < 12 mm; ++: growth zones 12–20 mm; +++: growth zones > 20 mm. The asterisks indicate a secondary growth zone to mycobactin after four additional days of growth at room temperature

Siderophores	*M. smegmatis* SG 987	*M. smegmatis* 987-M10	*M. fortuitum* ATCC 6841
Enterobactin	–	–	–
Myxochelin C	+++	+++	+++
Serratiochelin	+++	+++*	+++
Chrysobactin	–	–	–
Ferrioxamine B	++	+	+
Ferrioxamine E	+	+	+
Ferrioxamine G	+	+	+
Ferrichrome	+	+	+
Ferricrocin	+++	+++*	+++
Rhodotorulic acid	+++	+++*	+++
Aerobactin	–	+	–
Coprogen	+	+	+
Pyoverdin	–	–	+
Azotobactin	–	–	+
Rhizoferrin	++	+	++
Citrate	++	+	++
2,3 DHBA	+	+	+
Salicylic acid	++	+	–
Mycobactin	+++	+++	+++
Mycoexochelin	+++	+++*	+++

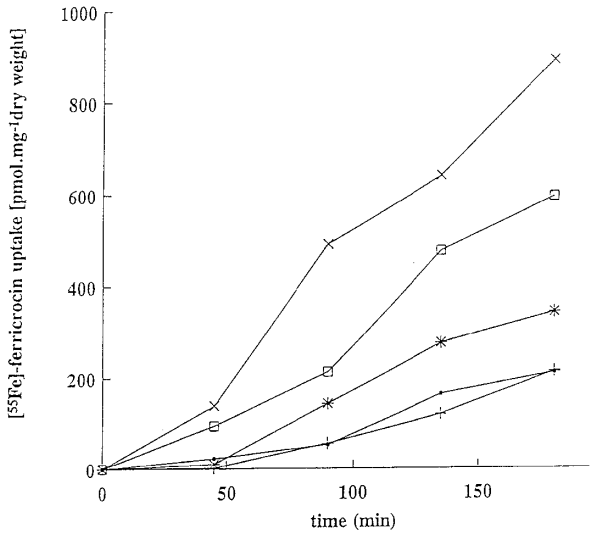

Figure 1. Time-dependent [^{55}Fe]ferricrocin uptake in *M. smegmatis* SG 987 at various siderophore concentrations (●, 10 μM; +, 20 mM; *, 40 μM; □, 80 μM; ×, 100 μM).

for the synthesis of an antibiotic derivative (antibiotic moiety attached to the siderophore via the peptide's serine OH). [^{55}Fe] ferricrocin transport was monitored in the time and concentration domain. Various growth conditions were tested for the uptake study (data not shown). Growth in complex medium followed by growth in MM followed by growth in low-iron MM yielded the best results. Figure 1 shows time-dependent uptake of ferricrocin at various concentrations. The time window for the transport assay was 3 h, which differs from other bacterial and fungal siderophore transport systems (4–15 min) indicating considerably lower uptake rates. The transport was effectively inhibited by the respiratory poison cyanide (100 μM). Similar results were achieved with the mutant 987-M10 (data not shown). If saturation kinetics of uptake are observed, the membrane transport can be formally analysed in terms of Michaelis–Menten constants. The concentration-dependent uptake rates of ferricrocin in *M. smegmatis* show saturation kinetics. A Lineweaver–Burk plot thereof ($r = 0.989$) yielded a maximum velocity v_{max} = 3.6 pmol mg^{-1} min^{-1} and an apparent K_m of = 24.82 μM. For the endogenous exochelin transport system of *M. smegmatis* a K_m of 6 μM was found (Stephenson & Ratledge 1979).

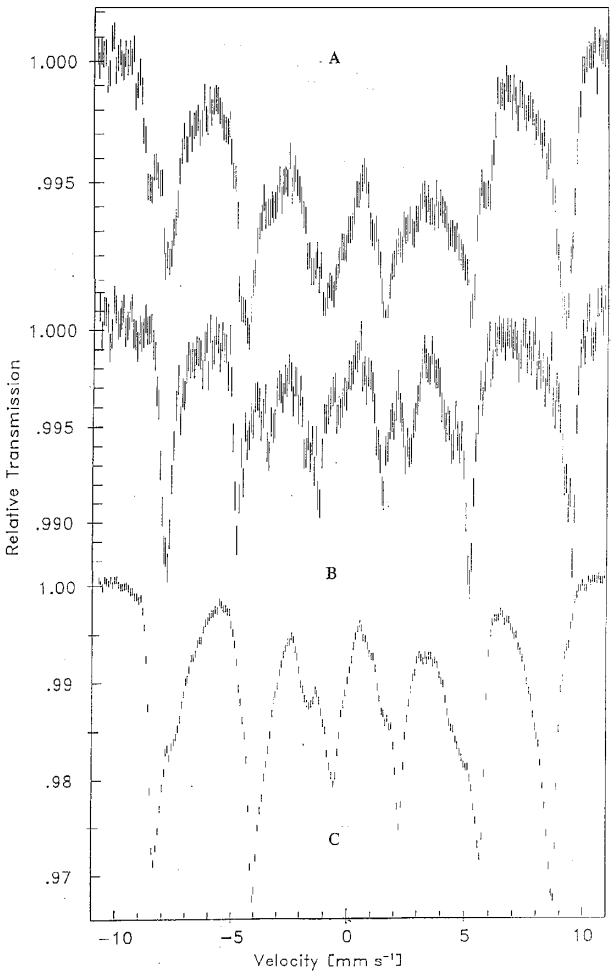

Figure 2. Mössbauer spectra of frozen methanolic solution of [^{57}Fe]-labelled mycobactin J (A) and of frozen aqueous solutions of ferricrocin (B) and ferric citrate (C). (B) was diluted with BSA in order to minimize spin–spin relaxation. The spectra were measured at 4.2 K in a magnetic field B_{app}= 20 mT perpendicular to the γ-beam.

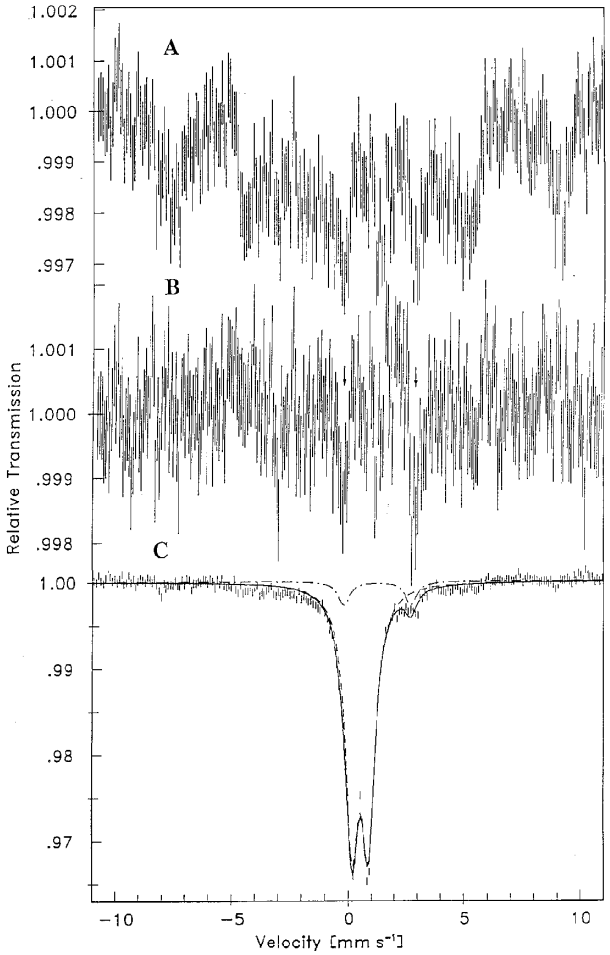

Figure 3. *In situ* Mössbauer spectra of frozen *M. smegmatis* SG 987 cells grown for six days in iron-deficient mineral salts medium and then incubated for 2 h with 20 μM [^{57}Fe](citrate)$_{-2}$(A). Spectrum (B) is spectrum (A) after subtracting the spectrum of mycobactin J (Figure 2A, 100% of the absorption area). Subtracting ferric citrate itself (Figure 2C) was not successful. In sample (C) 20 μM [^{57}Fe](citrate)$_2$ was added to the inoculum. Mössbauer spectra were measured at 4.2 K in a perpendicular field of 20 mT. Solid and broken lines are obtained by least-squares fits of Lorentzian lines to the experimental spectra yielding the Mössbauer parameters mentioned in the text.

In situ *[^{57}Fe] Mössbauer and EPR spectroscopy*

Ferricrocin-mediated iron uptake and metabolization in *M. smegmatis* SG 987 was followed by [^{57}Fe] Mössbauer and EPR spectroscopy. For comparison we also analysed citrate-mediated [^{57}Fe] transport. Figure 2 displays the Mössbauer spectra of frozen aqueous solutions of [^{57}Fe](citrate)$_2$ (1/20), of [^{57}Fe] ferricrocin and of methanolic [^{57}Fe]mycobactin J at 4.2 K. The spectra are typical for Fe(III) S=5/2 systems in the slow relaxation limit. In the case of ferricrocin spin–spin relaxation was minimized by BSA. The overall magnetic splittings of the three complexes differ, i.e. 51.1 T(ferricrocin), 50.6 T (mycobactin) and 47.2 T (ferric citrate), enabling their discrimination in cell spectra.

Figure 3A shows a Mössbauer spectrum of *M. smegmatis* grown for six days in iron-deficient medium and incubated for 2 h with [^{57}Fe](citrate)$_2$. Only very little iron is accumulated in the cells. The cell spectrum is dominated by a magnetically split species. This species could be subtracted using the experimental spectrum of mycobactin J (Figure 2A) yielding the spectrum depicted in Figure 3B. Attempts to subtract the magnetic species by using

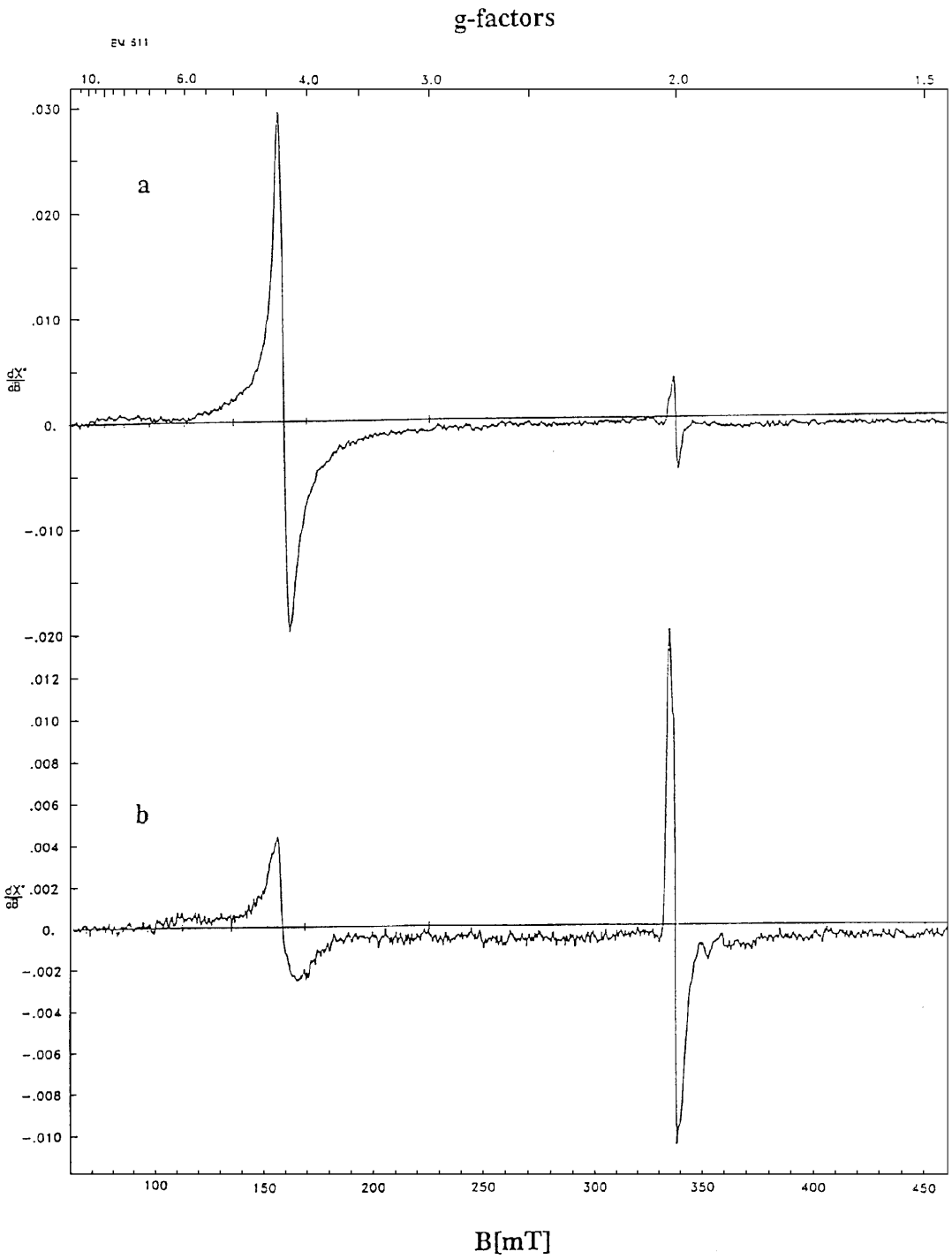

Figure 4. EPR spectra of frozen *M. smegmatis* SG 987 cells grown for six days in iron-deficient mineral salts medium. Spectrum (a) corresponds to the Mössbauer spectrum shown in Figure 3A. Spectrum (b) was measured from a long-term ferric citrate accumulation sample as in Figure 3C. Cells were measured at 10 K (microwave frequency, 9.431 GHz; microwave power, 20μW/40 dB; modulation frequency, 100 kHz; modulation amplitude, 1mT). The signal at $g = 4.3$ has been attributed to mycobactin, the signal at $g = 2$ represents an hitherto unidentified spin system, which, however, does not correspond to the Mössbauer species.

the spectrum of ferric citrate were not successful. Consequently, we attribute the magnetic species of the cell spectrum to mycobactin. The residual spectrum in Figure 3B indicates the presence of traces of ferrous iron (arrows). Figure 3C displays the spectrum of cells grown for six days with ferric citrate. Two components can be discriminated. The major species accounting for 92% of the experimental area exhibits Mössbauer parameters which are similar to *E.coli*-type bacterioferritin (numbers in parentheses): δ =0.53 (0.52) mm s^{-1}, ΔE_Q= 0.71 (0.65) mm s^{-1} (Bauminger *et al.* 1980, Andrews *et al.* 1991, Matzanke 1994, Pessolini *et al.* 1994). The second species accounts for 8% of the total absorption area and its Mössbauer parameters correspond to high-spin Fe(II): δ= 1.26 mm s^{-1}, ΔE_Q= 2.91 mm s^{-1}. Small indents at –8 mm s^{-1} and near +9 mm s^{-1} might indicate residual traces of mycobactin.

For comparison we have performed *in situ* EPR spectroscopy of cell samples prepared under the same conditions as for Mössbauer spectroscopy. The corresponding spectra recorded at 10 K are displayed in Figure 4. Only two signals are visible after short-term uptake (a) and after six days growth on ferric citrate (b). The signal at g = 4.3 is typical of rhombic iron as found in siderophores and many other ferric iron compounds. This signal decreases considerably in the long-term accumulation experiment. Based on the Mössbauer data we attribute this signal to mycobactin. The spectral feature around g = 2 is caused by a radical signal at g = 2.002 superimposed by a signal with two visible g values at 2.02 and 1.92 which might arise from a Fe–S cluster. This latter signal increases with growth time. To estimate whether this signal can be explained by the loss of the mycobactin signal at 4.3, relative spin concentrations were determined by double integration of the EPR pattern and by applying the correction factors of Åasa and Vänngård (1975) for field swept EPR pattern. The signal intensity of the whole feature around g = 2 increases by a factor of 0.7 after six days growth on ferric citrate. However, this factor does not correlate with the loss of the signal intensity of the mycobactin signal which would account for a 42-fold increase. Moreover, the relative area of the Mössbauer spectrum increases in the same time by a factor of 10. Therefore, the EPR spectrum of Figure 4b represents a minute amount of total cellular iron. From the Mössbauer spectra it is clear that much more iron is accumulated in sample (b) than in sample (a) (Figures 3A and C). Moreover, the Mössbauer parameters correspond to *E.coli*-type bacterioferritin. The formation of bacterioferritin

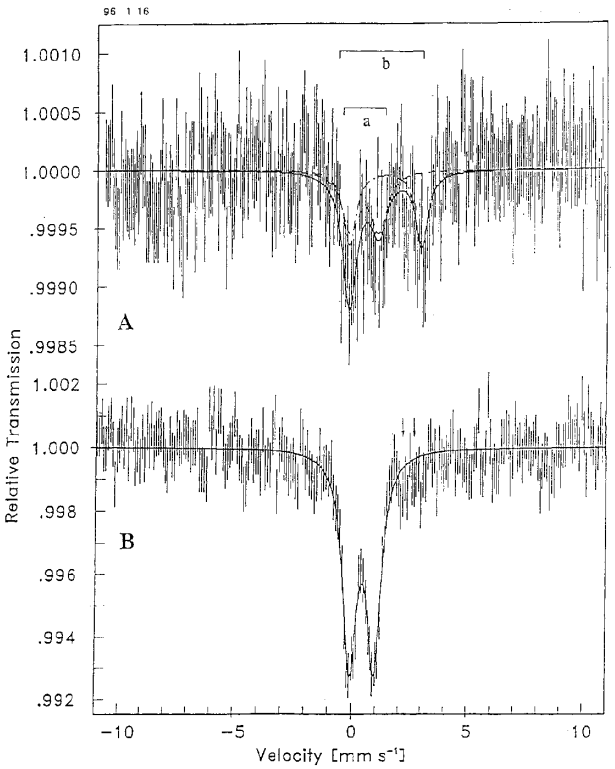

Figure 5. *In situ* Mössbauer spectra of frozen *M. smegmatis* SG 987 cells grown for six days in iron-deficient mineral salts medium and then incubated for 2 h with 20 μM [^{57}Fe]ferricrocin (A). In sample (B) 20 μM [^{57}Fe]ferricrocin was added to the inoculum. The experimental conditions were the same as described in Figure 3. The subspectra (a) and (b) in Figure 5A correspond to ferric (δ = 0.47 mm s^{-1}, ΔE_Q= 1.10 mm s^{-1}, 45% of total absorption area) and a ferrous iron species (δ= 1.32 mm s^{-1}, ΔE_Q= 3.13 mm s^{-1}, 55% of total absorption area). The arrows in Figure 5B indicate the possible presence of traces of ferrous iron.

as derived from the Mössbauer spectrum is corroborated by the effective loss of spin density in the EPR spectrum, because ferromagnetic resonance of superparamagnetic iron clusters at low temperatures yields very broad line widths (Boas & Troup 1971).

It has previously been suggested, but not proven, that exogenous iron bound to citrate is transferred to membrane-bound mycobactin which would act as an iron storage compound (Messenger & Ratledge 1982, Ratledge *et al.* 1982). In this work we present for the first time direct evidence that there is indeed a transfer of iron to mycobactin. In addition we have found a ferrous ion metabolite similar to other microorganisms (Matzanke *et al.* 1989b, 1991a,b, Böhnke & Matzanke 1995). However, in the long-

term iron accumulation mycobactin disappears and a bacterioferritin-like compound is found. Based on these findings a merely transient role has to be attributed to mycobactin. The ultimate storage compound is bacterioferritin which has indeed been isolated as a major membrane protein from various mycobacteria during the course of this project (Inglis *et al.* 1994, Pessolini *et al.* 1994). Over 90% of the cellular iron is stored in this membrane-bound bacterioferritin.

Exochelin transport in mycobacteria is thought to involve reductive removal of the metal on the cytoplasmic side of the membrane, whereas mycobactin serves merely as an overflow iron repository (Wheeler & Ratledge 1994). The citrate-mediated iron accumulation seems to be distinct (although we cannot completely exclude citrate/exochelin ligand exchange in the medium). Three series of events are possible:

i) ferric citrate → mycobactin(membrane-bound) → Fe(II) → bacterioferritin

ii) ferric citrate → Fe(II) → mycobactin → bacterioferritin

iii) ferric citrate → Fe(II) → mycobactin → Fe(II)′ → bacterioferritin.

We assume that route (iii) is not very likely because two energy-consuming Fe(III)/Fe(II) redox cycles are required compared to one in routes (i) and (ii). Route (ii) is not consistent with our data because a decrease in the cellular ferrous iron concentration, but not disappearance of mycobactin, should be expected in this model. Moreover, iron binding to mycobactin is tight and a non-reductive release of Fe(III) to ferritin is thermodynamically not favoured. Therefore, we suggest the ligand exchange route (i), because this model fits best with our data and with our current state of knowledge about the mechanism of iron-core formation in ferritin via ferrous iron (Bauminger *et al.* 1989, Jacobs *et al.* 1989, Levi *et al.* 1992, Treffry *et al.* 1992).

Figure 5 shows *in situ* Mössbauer spectra of [^{57}Fe] ferricrocin-mediated iron accumulation in *M. smegmatis* SG 987. Again, in the short-term uptake experiment (2 h) very little accumulation is found, which is in agreement with the [^{55}Fe] uptake data. No magnetically split species could be detected excluding the possibility of ferricrocin accumulation or ligand exchange involving mycobactin as takes place in the case of [^{57}Fe](citrate)$_2$ uptake. Two species can be discriminated, namely a ferrous iron (δ= 1.32 mm s^{-1}, ΔE_Q= 3.13 mm s^{-1}, 55% of total absorption area) and a species exhibiting the parameters δ= 0.47 mm s^{-1}, ΔE_Q= 1.10 mm s^{-1}, 45% of total absorption area. In the long-term experiment (Figure 5B) only one cellular iron compound can be detected. The concentrations of all other cellular iron species are below the detection limit, i.e. below 1% of the total cellular iron pool. The Mössbauer parameters (δ= 0.43 mm s^{-1}, ΔE_Q= 1.03 mm s^{-1}) are very close to the ferric iron species in spectrum (a) of Figure 5A, and we attribute both subspectra to the same intracellular compound. Obviously no iron or merely traces of it are transferred to ferritin under ferricrocin-controlled growth. Small inflections near 2 mm s^{-1} and 3 mm s^{-1} (arrows in Figure 5B) may indicate the presence of traces of ferrous iron species.

Since no sextet component is visible in the cell spectra after short-term uptake, we conclude that ferricrocin is apparently not accumulated in *M.smegmatis*. This indicates a rapid metal transfer. After short-term uptake ferrous iron accounts for approximately 55% of the total absorption area whereas its contribution is vanishing after six days growth with ferricrocin. This decrease of ferrous iron, together with similar findings in recent Mössbauer studies of siderophore uptake in a broad variety of microorganisms, strongly suggests that ferricrocin uptake in *M. smegmatis* is followed by reductive removal of the metal which is then converted to the ferric component (Matzanke 1991, Matzanke *et al.* 1991a, b). In the case of *E.coli* the ferrous iron compound has been isolated. It is an oligomeric sugar phosphate and has been termed ferrochelatin (Böhnke & Matzanke 1995). The ferric iron species detected after ferricrocin-mediated iron transport has been found in cell spectra of many microorganisms like *E. coli, Pantoea, Neurospora and Rhodotorula* (Matzanke 1991, Matzanke *et al.* 1991a,b). The corresponding compound has not yet been isolated or biochemically characterized. Its Mössbauer parameters do not fit those of bacterioferritin, cytochromes or iron–sulfur clusters.

Whereas citrate-mediated iron accumulation in *M. smegmatis* is linked to mycobactin and eventually to bacterioferritin iron-core formation, the metal transfer following ferricrocin uptake is strikingly different. A rapid reductive ligand exchange (probably to ferrochelatin) is suggested followed by the formation of a hitherto uncharacterized ferric iron compound. Whether ferricrocin enters the cytoplasmic side of the cell membrane before reduction or whether the reduction occurs at the membrane level remains unclear. However, neither ferricrocin nor mycobactin accumulation inside the cell can be

observed. No bacterioferritin iron cores are formed and very little – if any – ferrous iron is found after long-term accumulation.

In summary, this study provides direct evidence for two different routes of intracellular iron transfer in mycobacteria. One route is associated with the iron chelator citrate exhibiting complex formation constants lower than that of mycobactin, and a second is associated with the siderophore ferricrocin exhibiting a similar or even higher complex formation constant than mycobactin. Nevertheless, for each group of compounds specific recognition at the membrane level and regulated transport is required, as can be derived from growth promotion tests.

Acknowledgements

This work was supported by BMBF grant No. 01KI9405 and by an EC stipend grant (CHRX CT94 0589; RB).

References

Åasa R, Vänngård T. 1975 EPR signal intensity and powder shapes: a reexamination. *J Magn Res* **19**, 308–315.

Andrews SC, Findlay JBC, Guest JR, *et al.* 1991 Physical, chemical and immunological properties of bacterioferritins of *Escherichia coli, Pseudomonas aeruginosa* and *Azotobacter vinelandii. Biochim Biophys Acta* **1078**, 111–116.

Bagg A, Neilands JB. 1987 Molecular mechanisms of regulation of siderophore mediated iron assimilation. *Microbiol Rev* **51**, 509–518.

Barclay R, Ratledge C. 1983 Iron-binding compounds of *Mycobacterium avium, M. intracellulare, M. scrofulaceum,* and mycobactin-dependent *M. paratuberculosis* and *M. avium. J Bacteriol* **153**, 1138–1146.

Bauminger ER, Cohen SG, Dickson DPE, *et al.* 1980 Mössbauer spectroscopy of *Escherichia coli* and its iron-storage protein. *Biochim Biophys Acta* **623**, 237– 242.

Bauminger ER, Harrison PM, Nowik I, Treffry A. 1989 Mössbauer spectroscopic study of the initial stages of iron-core formation in horse spleen apoferritin; evidence for both isolated Fe(III) atoms and oxo-bridged Fe(III) dimers as early intermediates. *Biochemistry* **28**, 5486–5493.

Bloom BR. 1992 Back to a frightening future. *Nature* **358**, 538–539.

Boas JF, Troup GJ. 1971 Electron spin resonance and Mössbauer effect studies of ferritin. *Biochim Biophys Acta* **229**, 68–74.

Böhnke R, Matzanke BF. 1995 The mobile ferrous iron pool in *Escherichia coli* is bound to a phosphorylated sugar derivative. *BioMetals* **8**, 223–230.

Braun V. 1981 *Escherichia coli* containing the plasmid ColV produce the iron ionophore aerobactin. *FEMS Microbiol Lett* **11**, 215–228.

Braun V, Hantke K. 1991 Genetics of bacterial iron transport. In: Winkelmann G, ed. *Handbook of Microbial Iron Chelates* (Siderphores). Boca Raton, FL: CRC Press; 107–138.

David HL. 1981 Basis for lack of drug susceptibility of atypical mycobacteria. *Rev Infect Dis* **3**, 878–884.

Ecker DJ, Matzanke BF, Raymond KN. 1986 Specificity of ferric enterobactin transport in *E.coli. J Bacteriol* **167**, 666–673.

Hall RM, Ratledge C. 1982 A simple method for the production of mycobactin, the lipid soluble siderophore, from bacteria. *FEMS Microbiol Lett* **15**, 133–136.

Hall RM, Ratledge C. 1987 Exochelin-mediated iron acquisition by the leprosy bacillus, *Mycobacterium leprae. J Gen Microbiol* **133**, 193–199.

Hall RM, Sritharan M, Messenger AJM, Ratledge C. 1987 Iron transport in *Mycobacterium smegmatis*: Occurrence of iron–regulated envelope proteins as potential receptors for iron uptake. *J Gen Microbiol* **133**, 2107–2114.

Inglis NF, Stevenson K, Hosie AH, Sharp JM. 1994 Complete sequence of the gene encoding the bacterioferritin subunit of *Mycobacterium avium* subspecies silvaticum. Gene **150**, 205–206.

Jacobs D, Watt GD, Frankel JB, Papaefthymiou GC. 1989 Fe^{2+} binding to apo and holo mammalian ferritin. *Biochemistry* **28**, 9216–9221.

Kaufmann SHE, van Embden JD. 1993 Tuberculosis; a neglected disease strikes back. *Trends Microbiol* **1**, 2–5.

Levi S, Yewdall SJ, Harrison PM, *et al.* 1992 Evidence that H- and L-chains have co-operative roles in the iron-uptake mechanism of human ferritin. *Biochem J* **288**, 591–597.

Macham LP, Ratledge C. 1975 A new group of water-soluble iron-binding compounds from mycobacteria; the exochelins. *J Gen Microbiol* **89**, 379–382.

Macham LP, Ratledge C, Nocton JC. 1975 Extracellular iron acquisition by mycobacteria; role of the exochelins and evidence against the participation of mycobactin. *Infection and Immunity* **12**, 1242–1251.

Matzanke BF. 1987 Mössbauer spectroscopy of microbial iron uptake and metabolism. In: Winkelmann G, van der Helm D, Neilands JB, eds. *Iron Transport in Microbes, Plants and Animals.* Weinheim, Germany: VCH; 251–284.

Matzanke BF. 1991 Structures, coordination chemistry and functions of microbial iron chelates. In: Winkelmann G, ed. *Handbook of Microbial Iron Chelates* (Siderophores). Boca Raton, FL: CRC Press; 15–60.

Matzanke BF. 1994 Iron storage in fungi. In: Winkelmann G, Wing DR, eds. *Metal Ions in Fungi.* NY: Marcel Dekker; 179–214.

Matzanke BF, Ecker DJ, Yang T-S, *et al*. 1986 Iron enterobactin uptake in *Escherichia coli* followed by Mössbauer spectroscopy. *J Bacteriol* **167**, 674–680.

Matzanke, BF, Müller-Matzanke G, Raymond KN. 1989a Siderophore mediated iron transport. In: Loehr TR, ed. *Iron Carriers and Iron Proteins*, New York, NY. VCH Publishers; 1–121.

Matzanke BF, Müller G, Bill E, Trautwein AX. 1989b Iron metabolism of *E.coli* studied by Mössbauer spectroscopy and biochemical methods. *Eur J Biochem* **183**, 371–379.

Matzanke BF, Berner I, Bill E, Trautwein AX, Winkelmann G. 1991a Iron transport and metabolism in *E. herbicola. Biol Met* **4**, 181–185.

Matzanke BF, Bill E, Trautwein AX. 1991b Main components of iron metabolism in microbial systems – analyzed by *in vivo* Mössbauer spectroscopy. *Hyperfine Interact* **71**, 1259–1262.

Messenger AJM, Ratledge C. 1982 Iron transport in *Mycobacterium smegmatis*: uptake of iron from ferric citrate. *J Bacteriol* **149**, 131–135

Müller G, Matzanke BF, Raymond KN. 1984 Iron transport in *Streptomyces pilosus* mediated by ferrichrome type siderophores, rhodotorulic acid and enantiorhodotorulic acid. *J Bacteriol* **160**, 313–318.

Neilands JB. 1982 Microbial iron transport compounds. In: Laskin AI, Lechevalier HA, eds. *Handbook of Microbiology*, Vol IV, 2nd ed. Boca Raton, FL: CRC Press; 565–574.

Neilands JB, Nakamuro K. 1991 Detection, determination, isolation, characterization and regulation of microbial iron chelates. In: Winkelmann G, ed. *Handbook of Microbial Iron Chelates* (Siderophores). Boca Raton, FL: CRC Press; 1–14.

Pessolini MC, Smith DR, Rivoire B, *et al*. 1994 Purification, characterization, gene sequence, and significance of a bacterioferritin from *Mycobacterium leprae*. *J Exp Med* **180**, 319–327.

Rastogi N. 1993 Emergence of multiple-drug-resistant tuberculosis: fundamental and applied research aspects, global issues and current strategies. *Res Microbiol* **144**, 103–121.

Ratledge C. 1964 Relationship between the products of aromatic biosynthesis in *Mycobacterium smegmatis* and *Aerobacter aerogenes*. *Nature* **203**, 428–429.

Ratledge C. 1982 Mycobactins and nocobactins. In: Laskin AI, Lechevalier HA, eds. *Handbook of Microbiology*, Vol IV, 2nd ed. Boca Raton, FL: CRC Press; 575–581.

Ratledge C, Chaudrey MA. 1971 Accumulation of iron-binding phenolic acids by actimycetales and other organisms related to mycobacteria, *J Gen Microbiol* **66**, 71–78.

Ratledge C, Hall MJ. 1971 Influence of metal ions on the formation of mycobactin and salicylic acid in *Mycobacterium smegmatis* grown in static culture. *J Bacteriol* **108**, 314–319.

Ratledge C, Patel PV, Mundy J. 1982 Iron transport in *Mycobacterium smegmatis*: The location of mycobactin by electron microscopy. *J Gen Microbiol* **128**, 1559–1565.

Raymond KN, Müller GI, Matzanke BF. 1984 Complexation of iron by siderophores. A review of their solution and structural chemistry and biological function. *Topics in Current Chemistry* **123**, 49–102.

Reissbrodt R, Rabsch A, Chapeaurouge A, Winkelmann G, Jung G. 1990 Isolation and identification of ferrioxamine G and E in *Hafnia alvei. Biol Metals* **3**, 54–60.

Reissbrodt R, Heinisch L, Möllmann U, Ulbricht H. 1993 Growth promotion of synthetic catecholate derivatives on Gram-negative bacteria. *BioMetals* **6**, 155–162.

Schwyn B, Neilands JB. 1987 Universal chemical assay for the detection and determination of siderophores. *Anal Biochem* **160**, 47–52.

Sharman GJ, Williams DH, Ewing DF, Ratledge C. 1995a Determination of the structure of exochelin MN, the extracellular siderophore from *Mycobacterium neoaurum. Curr Biol* **2**, 553–561.

Sharman GJ, Williams DH, Ewing DF, Ratledge C. 1995b. Isolation, purification and structure of exochelin MS, the extracellular siderophore from *Mycobacterium smegmatis*. *Biochem J* **305**, 187–196.

Snow GA. 1970 Mycobactins: Iron-chelating growth factors from mycobacteria. *Bacteriol Rev* **34**, 99–125.

Stephenson MC, Ratledge C. 1979 Iron transport in *Mycobacterium smegmatis*: uptake of iron from ferriexochelin. *J Gen Microbiol* **110**, 193–202.

Thieken A, Winkelmann G. 1992 Rhizoferrin; A complexone type siderophore of the Mucorales and Entomophtorales (Zygomycetes). *FEMS Microbiol Lett* **94**, 37–42.

Treffry A, Hirzmann J, Yewdall SJ, Harrison PM. 1992 Mechanism of catalysis of Fe(II) oxidation by ferritin H chains. *FEBS Letters* **302**, 108–112.

Trowitzsch-Kienast W, Hartmann V, Reissbrodt R, Ambrosi HD. 1994 Myxochelin C und verwandte Verbindungen, neue Syntheseprodukte als Metalltransporteure und als Chemo-therapeutische Mittel. Patent pending at the German Patents Agency, file number 4447374.5.

WHO Press release 31. 1993 In: *Bundesgesundheitsblatt* **8**, 337.

Wheeler PR, Ratledge C. 1994 Metabolism of *Mycobacterium tuberculosis*. In: Bloom BR, ed. *Tuberculosis*. Washington, DC: ASM Press; 353–388.

Winkelmann G. 1986 Iron complex products. In: Rehm H-J, Reed G, eds. *Biotechnology*, Vol. 4. Weinheim FRG: VCH Verlagsgesellschaft; 215–243.

Winkelmann G. 1991 Specificity of iron transport in bacteria and fungi. In: Winkelmann G, ed. *Handbook of Microbial Iron Chelates* (Siderophores). Boca Raton, FL: CRC Press; 65–105.

Wong GB, Kappel MJ, Raymond KN, Matzanke B, Winkelmann G. 1983 Coordination chemistry of microbial iron transport compounds. 24. Characterization of coprogen and ferricrocin, two ferric hydroxamate siderophores. *J Am Chem Soc* **105**, 810–815.

Zhang Y, Heym B, Allen B, Young D, Cole S. 1992 The catalase-peroxidase gene and isoniazid resistance of *Mycobacterium tuberculosis. Nature* **358**, 591–593.